original reports

Association Between Brain Substructure Dose and Cognitive Outcomes in Children With Medulloblastoma Treated on SJMB03: A Step Toward Substructure-Informed Planning

Sahaja Acharya, MD[1,2]; Yian Guo, MS[3]; Tushar Patni, MS[3]; Yimei Li, PhD[3]; Chuang Wang, PhD[1]; Melissa Gargone, MHS[1]; Jason M. Ashford, MS[4]; Lydia Wilson, PhD[1]; Austin Faught, PhD[1]; Wilburn E. Reddick, PhD[5]; Zoltan Patay, MD, PhD[5]; Amar Gajjar, MD[6]; Heather M. Conklin, PhD[4]; and Thomas E. Merchant, DO, PhD[1]

abstract

PURPOSE To characterize the association between neurocognitive outcomes (memory and processing speed) and radiation (RT) dose to the hippocampus, corpus callosum (CC), and frontal white matter (WM) in children with medulloblastoma treated on a prospective study, SJMB03.

PATIENTS AND METHODS Patients age 3-21 years with medulloblastoma were treated at a single institution on a phase III study. The craniospinal RT dose was 23.4 Gy for average-risk patients and 36-39.6 Gy for high-risk patients. The boost dose was 55.8 Gy to the tumor bed. Patients underwent cognitive testing at baseline and once yearly for 5 years. Performance on tests of memory (associative memory and working memory) and processing speed (composite processing speed and perceptual speed) was analyzed. Mixed-effects models were used to estimate longitudinal trends in neurocognitive outcomes. Reliable change index and logistic regression were used to define clinically meaningful neurocognitive decline and identify variables associated with decline.

RESULTS One hundred and twenty-four patients were eligible for inclusion, with a median neurocognitive follow-up of 5 years. Mean right and left hippocampal doses were significantly associated with decline in associative memory in patients without posterior fossa syndrome (all $P < .05$). Mean CC and frontal WM doses were significantly associated with decline in both measures of processing speed (all $P < .05$). Median brain substructure dose–volume histograms were shifted to the right for patients with a decline in associative memory or processing speed. The odds of decline in associative memory and composite processing speed increased by 23%-26% and by 10%-15% for every 1-Gy increase in mean hippocampal dose and mean CC or frontal WM dose, respectively.

CONCLUSION Increasing RT dose to the CC or frontal WM and hippocampus is associated with worse performance on tests of processing speed and associative memory, respectively. Brain substructure–informed RT planning may mitigate neurocognitive impairment.

J Clin Oncol 40:83-95. © 2021 by American Society of Clinical Oncology

ASSOCIATED CONTENT

Appendix

Protocol

Author affiliations and support information (if applicable) appear at the end of this article.

Accepted on September 29, 2021 and published at ascopubs.org/journal/jco on October 29, 2021: DOI https://doi.org/10.1200/JCO.21.01480

INTRODUCTION

Medulloblastoma survivors are at risk for cognitive impairment secondary to treatment-related and disease-related factors. Treatment entails maximal safe resection, craniospinal irradiation (CSI) with a boost to the primary tumor bed, and chemotherapy.[1] Higher CSI doses and younger age at treatment are associated with poorer cognitive outcomes.[2] The effects of neurocognitive impairment are pervasive, affecting academic performance,[3] social-emotional functioning,[4] and the ability to live independently as an adult.[5]

The hippocampus and white matter (WM) are particularly vulnerable to radiation (RT) injury. The hippocampus plays a primary role in encoding new memories,[6-8] and neurogenesis within the hippocampus is impaired after cranial irradiation.[9-11] Hippocampal avoidance in adults undergoing whole-brain RT has resulted in better memory preservation when compared with standard of care.[12] In children with low-grade brain tumors, increased hippocampal dose is associated with worse memory performance.[13,14] With respect to WM, there is a correlation between decreased WM integrity and RT dose, with the largest changes occurring in the corpus callosum (CC) and frontal WM.[15-17] Decreased WM integrity within these regions correlates with specific neurocognitive domains, such as attention and processing speed.[17,18] Overall, these data suggest that the hippocampus, CC,

CONTEXT

Key Objective

Medulloblastoma survivors are at risk for cognitive impairment secondary to radiation (RT). Brain substructures such as the hippocampus, corpus callosum (CC), and frontal white matter (WM) are particularly vulnerable to RT injury and are associated with specific neurocognitive functions. Using data from SJMB03, a phase III study in which children with histologically confirmed medulloblastoma received craniospinal RT, we investigated the relation between the following: (1) hippocampal dose and memory, (2) CC dose and processing speed, and (3) frontal WM dose and processing speed.

Knowledge Generated

Higher mean dose to the hippocampi and CC or frontal WM was associated with worse performance on tests of associative memory and processing speed, respectively.

Relevance

This study sets the stage for implementing substructure-informed RT planning in future medulloblastoma protocols with the goal of reducing deficits in memory and processing speed, ultimately improving the quality of life of medulloblastoma survivors.

and frontal WM are particularly vulnerable to injury from RT and are associated with specific neurocognitive functions.

The increased conformality of modern RT techniques and the reduction in medulloblastoma boost volume from whole posterior fossa to tumor bed provide an opportunity to minimize RT injury to brain substructures critical for neurocognitive function.[19] A better understanding of the relation between dose to brain substructures and cognitive outcomes in children will result in RT plans that are optimized to preserve neurocognition. The primary aim of this study was to use data from SJMB03 (ClinicalTrials.gov identifier: NCT00085202), a phase III study in which children with histologically confirmed medulloblastoma received CSI with a focal boost to the tumor bed, to investigate the relation between the following: (1) hippocampal dose and memory, (2) CC dose and processing speed, and (3) frontal WM dose and processing speed. We hypothesized that increasing dose to the hippocampus and CC or frontal WM would adversely affect memory and processing speed, respectively. The secondary aim was to understand how RT affected the growth of these substructures by comparing volumetric change in patients with that in healthy participants.

PATIENTS AND METHODS

Study Population

SJMB03 patients. Eligible patients included children with medulloblastoma who were age 3-21 years at diagnosis and were enrolled on SJMB03 at St Jude Children's Research Hospital (St Jude; N = 155; Appendix Fig A1, online only). Patients were enrolled at St Jude from September 2003 to June 2013. Patients enrolled and treated at non-St Jude sites were not included in this study. SJMB03 trial schema and eligibility criteria have been reported previously.[20] In brief, patients with average-risk disease (M0 and gross total volume or near total volume) received 23.4 Gy of CSI and those with high-risk disease (M+ or subtotal volume) received 36-39.6 Gy of CSI. All patients received photon therapy, with a 55.8 Gy boost to the tumor bed, using a 1-cm clinical target volume margin. Magnetic resonance imaging (MRI; T1, T2, and/or fluid-attenuated inversion recovery) was used to define the boost target. Metastases > 0.5 cm received a boost of 50.4-54 Gy. One high-risk patient was treated to 41.4 Gy CSI because of extensive metastases. All patients received adjuvant chemotherapy, scheduled 6 weeks after completion of RT and consisting of four cycles of high-dose cyclophosphamide, cisplatin, and vincristine with stem-cell support. The following clinical variables were extracted from the medical record database: age at study enrollment, sex, number of surgeries, completion of adjuvant chemotherapy, presence of hydrocephalus (defined as requiring a shunt, external ventricular drain, or endoscopic third ventriculostomy), hearing loss (defined as > 25 dB of hearing loss at 2,000 Hz), posterior fossa syndrome (PFS; defined according to the 2016 Iceland Delphi Consensus Conference),[21] median household income on the basis of residential zip code (estimated using 2006-2010 data from the American Community Survey[22]), and molecular subgroup (determined by DNA methylation–based classification[23]).

Patients were excluded if the cumulative RT plan (CSI and boost) could not be retrieved (n = 14); if the baseline pre-RT MRI scan was of poor quality, preventing delineation of brain substructures (n = 5); or if the patient had completed fewer than two neurocognitive evaluations (n = 12; Appendix Fig A1).

SJMB03 was approved by the St Jude Institutional Review Board. Written informed consent was obtained from patients, parents, or guardians.

Healthy participants. Eligible participants were age 6-25 years and had no major psychiatric, neurologic, or medical diagnoses. Participants were enrolled from October 16,

TABLE 1. Characteristics of SJMB03 Patients and Healthy Participants

Variable	SJMB03	Healthy Participants
Total No. of patients or children	124	82
Sex, No. (%)		
Female	46 (37)	34 (41)
Male	78 (63)	48 (59)
Median age in years at enrollment (range)	9 (3-21)	13 (6-25)
Hydrocephalus, No. (%)		
No	60 (48)	
Yes	64 (52)	
No. of surgeries, No. (%)		
1	98 (79)	
2	24 (19)	
> 2	2 (2)	
Posterior fossa syndrome, No. (%)		
No	101 (81)	
Yes	23 (19)	
Craniospinal dose, Gy, No. (%)		
23.4	84 (68)	
36	25 (20)	
39.6	14 (11)	
41.4	1 (1)	
Boost to intracranial metastatic disease, No. (%)		
No	108 (87)	
Yes	16 (13)	
Sites of intracranial metastatic boost,[a] No. (%)		
Suprasellar or infundibulum	11 (58)	
Frontal lobe	3 (16)	
Occipital lobe	2 (11)	
Pineal region	2 (11)	
Internal auditory canal	1 (5)	
Completion of adjuvant chemotherapy, No. (%)		
Yes	117 (6)	
No	7 (6)	
Hearing loss, No. (%)		
No	103 (83)	
Yes	21 (17)	
Molecular subgroup, No. (%)		
WNT	18 (14)	
SHH	19 (15)	
Group 3 or 4	74 (61)	
Unknown	13 (10)	
Median household income,[b] $	48,601	

Abbreviations: SHH, sonic hedgehog; WNT, wingless.

[a]Patients may have more than one intracranial metastatic boost site.

[b]Median household income is based on zip code and estimated using data from the American Community Survey.

2007, to June 08, 2010, with a sex bias to match the patient population, and were recruited from the community. They were scheduled for three yearly noncontrast MRI scans (years 1, 2, and 3) without anesthesia. Written informed consent was obtained from participants, parents, or guardians. The imaging Protocol (online only) was approved by the St Jude Institutional Review Board.

Dose and Volume Analysis

Dose–volume histogram (DVH) data were extracted from cumulative RT plans. Each substructure was contoured on the postoperative pre-RT MRI, and the MRI was fused to the simulation CT. Contours were primarily based on three-dimensional (3D) T1 postcontrast MRI sequences. The hippocampus and CC were contoured according to the RTOG 0933 atlas and published guidelines,[24] respectively, by a board-certified RT oncologist. Frontal WM was auto-segmented using FreeSurfer Software[25] (Laboratory for Computational Neuroimaging at the Athinoula A. Martinos Center for Biomedical Imaging; Boston, MA) and verified manually.

For volumetric analysis of the SJMB03 population, the 2-year follow-up 3D T1 postcontrast MRI sequence was used for contouring if the image quality was adequate (n = 101). For volumetric analysis of healthy participants, 3D T1 noncontrast MRI sequences were used for contouring if image quality was adequate and both years 1 and 2 or years 1 and 3 scans were available (n = 82). The slice thickness was ≤ 1 mm for all MRI scans.

Neurocognitive Assessment

Patients underwent neurocognitive testing at baseline, defined as after surgical resection and before completion of RT, and once yearly for 5 years. The testing battery was consistent across all time points, and the results from the full battery have been reported previously.[2,26] For this study, specific measures from the Woodcock–Johnson Tests of Cognitive Abilities, Third Edition,[27] were chosen to characterize memory and processing speed. For memory, these measures included Visual Auditory Learning (associative memory) and Numbers Reversed (working memory). For processing speed, these measures included Visual Matching (perceptual speed) and a composite measure of processing speed that combined Visual Matching and Decision Speed (semantic processing speed). Age-adjusted standard scores on the basis of a large, representative normative sample have a population mean of 100 and a standard deviation (SD) of 15. Lower scores indicate worse performance. Patients with progressive disease discontinued protocol-based neurocognitive testing.

Statistical Analysis

Association between cognitive function, brain substructure dose, and clinical variables. The outcome variable was neurocognitive performance, as described above. Follow-up time was calculated from RT start to the last

neurocognitive test. Neurocognitive evaluations completed after disease progression were excluded from the analysis. Linear mixed-effects models were used to estimate longitudinal trends in these neurocognitive outcomes over time. Each patient was treated as a cluster, and the intercept was assumed to be random among patients. First, a series of univariable linear mixed-effects models were built for each covariate separately. These models included covariates and covariate-by-time interaction terms (slope). Second, clinical covariates and their interactions with time were included in the multivariable model if their interactions with time were significant on the first step ($P < .05$); however, age was always included in the multivariable model. Additionally, if the interaction of a dosimetric covariate with time was significant on univariate analysis ($P < .05$), it was carried forward to the multivariable model. Separate multivariable models were created for the right and left hippocampus, the right and left frontal WM, and the subdivisions of the CC (genu, body, and splenium). For each substructure, the Akaike information criterion (AIC) and Bayesian information criterion (BIC) were used to compare multivariable models with different dosimetric parameters (ie, the mean dose [D_{mean}] and the volumes receiving 30, 35, 40, and 45 Gy), with lower AIC and BIC values indicating better models. The multivariable model with D_{mean} resulted in the lowest AIC and BIC for each substructure, and a final stepwise selection was conducted to remove covariate(s) that turned insignificant in the multivariable model.

Association between substructure D_{mean} and clinically meaningful neurocognitive decline. Because many factors can affect neurocognitive scores on repetitive testing, the reliable change index (RCI) was used to identify patients with a clinically meaningful decline from baseline for each neurocognitive measure.[28,29] RCI was calculated as follows:

$$\text{RCI} = \frac{T_1 - T_2}{\text{SED}},$$

where SED is the SE of difference calculated from the SD of the test and the test reliability coefficient,[27] T_1 is the baseline score, and T_2 is the score at last neurocognitive

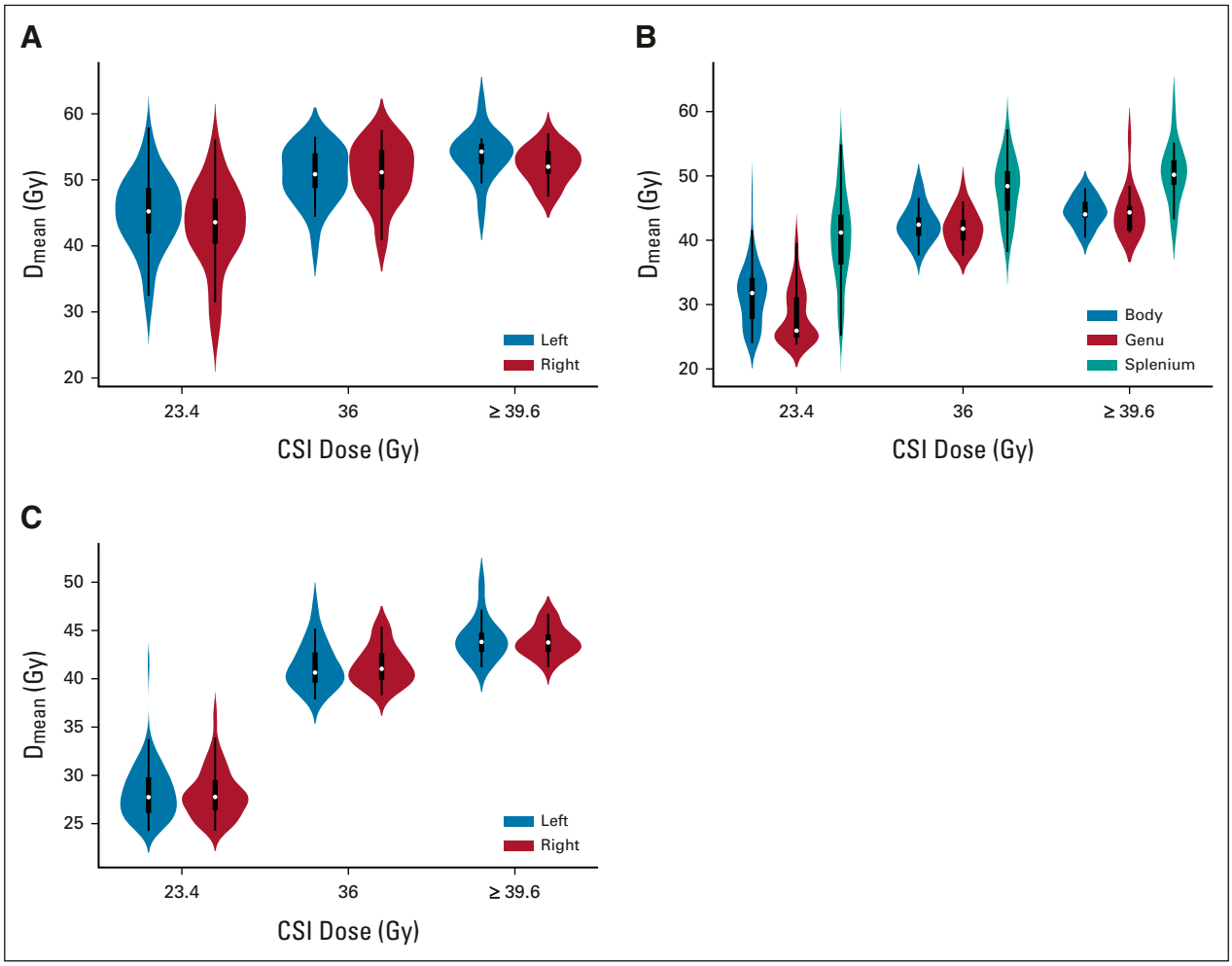

FIG 1. Violin plots of D_{mean} to (A) the hippocampus, (B) the CC, and (C) the frontal WM, stratified by craniospinal dose. CC, corpus callosum; CSI, craniospinal irradiation; D_{mean}, mean dose; WM, white matter.

TABLE 2. Parameter Estimates of Multivariable Linear Mixed Models Investigating the Associations of Brain Substructure Mean Dose, Age, and Sex With Longitudinal Trends in Different Neurocognitive Outcomes

Variable	No. of Patients	No. of Observations	Estimate	SE	*P*
Associative memory (no PFS)	99	453			
Left hippocampus					
Intercept			81.683	12.071	< .001
Sex			8.179	2.716	.003
Time			3.842	2.368	.106
Left D_{mean}			0.293	0.235	.216
Age			–0.369	0.325	.257
Left D_{mean} × time			–0.109	0.046	.019
Age × time			0.188	0.065	.004
Right hippocampus					
Intercept			91.539	10.567	< .001
Sex			8.737	2.734	.002
Time			3.803	2.238	.090
Right D_{mean}			0.093	0.210	.658
Age			–0.432	0.324	.185
Right D_{mean} × time			–0.110	0.044	.013
Age × time			0.182	0.065	.005
Working memory	117	524			
Intercept			96.624	3.843	< .001
Time			–2.544	0.753	.001
Age			–0.236	0.331	.478
Sex			4.611	2.910	.115
Age × time			0.232	0.062	< .001
Sex × time			–1.244	0.555	.025
Composite processing speed	122	629			
CC genu					
Intercept			76.352	9.547	< .001
Time			1.217	1.073	.258
D_{mean}			0.241	0.234	.304
Age			–0.225	0.423	.597
D_{mean} × time			–0.166	0.026	< .001
Age × time			0.441	0.048	< .001
CC body					
Intercept			77.968	10.798	< .001
Time			1.755	1.199	.144
D_{mean}			0.188	0.262	.475
Age			–0.260	0.420	.536
D_{mean} × time			–0.176	0.029	< .001
Age × time			0.464	0.047	< .001
CC splenium					
Intercept			77.457	11.943	< .001
Time			0.375	1.360	.783
D_{mean}			0.169	0.250	.499

(continued on following page)

TABLE 2. Parameter Estimates of Multivariable Linear Mixed Models Investigating the Associations of Brain Substructure Mean Dose, Age, and Sex With Longitudinal Trends in Different Neurocognitive Outcomes (continued)

Variable	No. of Patients	No. of Observations	Estimate	SE	*P*
Age			–0.268	0.416	.521
D_{mean} × time			–0.115	0.028	< .001
Age × time			0.472	0.048	< .001
Left frontal WM					
Intercept			71.765	10.213	< .001
Time			1.553	1.146	.176
D_{mean}			0.371	0.258	.152
Age			–0.193	0.424	.649
D_{mean} × time			–0.178	0.029	< .001
Age × time			0.444	0.048	< .001
Right frontal WM					
Intercept			72.416	10.132	< .001
Time			1.750	1.141	.126
Right D_{mean}			0.357	0.259	.170
Age			–0.206	0.422	.626
D_{mean} × time			–0.185	0.029	< .001
Age × time			0.445	0.048	< .001
Perceptual speed	122	644			
CC genu					
Intercept			72.432	9.420	< .001
Time			0.516	1.142	.651
D_{mean}			0.369	0.231	.112
Age			–0.274	0.418	.513
D_{mean} × time			–0.179	0.028	< .001
Age × time			0.451	0.051	< .001
CC body					
Intercept			74.034	10.682	< .001
Time			1.001	1.279	.434
D_{mean}			0.311	0.260	.233
Age			–0.323	0.415	.438
D_{mean} × time			–0.187	0.031	< .001
Age × time			0.474	0.051	< .001
CC splenium					
Intercept			75.540	11.806	< .001
Time			–0.439	1.457	.763
D_{mean}			0.227	0.247	.359
Age			–0.347	0.411	0.401
D_{mean} × time			–0.122	0.030	< .001
Age × time			0.480	0.052	< .001
Left frontal WM					
Intercept			68.033	10.058	< .001
Time			0.871	1.218	.475
Left D_{mean}			0.495	0.254	.053

(continued on following page)

TABLE 2. Parameter Estimates of Multivariable Linear Mixed Models Investigating the Associations of Brain Substructure Mean Dose, Age, and Sex With Longitudinal Trends in Different Neurocognitive Outcomes (continued)

Variable	No. of Patients	No. of Observations	Estimate	SE	*P*
Age			–0.248	0.417	.553
D_{mean} × time			–0.191	0.031	< .001
Age × time			0.453	0.051	< .001
Right frontal WM					
Intercept			68.261	9.984	< .001
Time			1.112	1.212	.359
D_{mean}			0.495	0.256	.055
Age			–0.261	0.416	.531
D_{mean} × time			–0.200	0.031	< .001
Age × time			0.454	0.051	< .001

Abbreviations: CC, corpus callosum; D_{mean}, mean dose; PFS, posterior fossa syndrome; WM, white matter.

follow-up. RCI results in a *z*-score similar to the SD index, and any score below –1.645 signifies a clinically meaningful decline.[29] Logistic regression was used to identify mean substructure doses associated with clinically meaningful declines. Only patients with both baseline and follow-up measurements were included in this analysis.

Comparing DVHs of patients with and without clinically meaningful neurocognitive decline. Permutation testing was performed to determine whether the median population DVH of patients with clinically meaningful neurocognitive decline was significantly different from that of patients without decline with an $\alpha = .05$ significance level (ie, $H_0: \widetilde{D_{Decline}} = \widetilde{D_{No\ decline}}$; $H_1: \widetilde{D_{Decline}} \neq \widetilde{D_{No\ decline}}$). Permutation testing enables multiple comparisons without the need for additional correction and provides a nonparametric method to establish statistical significance.[30-32] Our permutation test compared the test statistic, T,

$$T = \sum_{D_i=0}^{D_{max}} \left(\widetilde{V_{Decline}}\ (D_i) - \widetilde{V_{No\ decline}}\ (D_i) \right),$$

where D_{max} is the maximum dose magnitude in the DVH and $\widetilde{V_{Decline}}\ (D_i)$ $\widetilde{V_{No\ decline}}\ (D_i)$ are the median cumulative volume magnitudes at D_i for the decline and no decline cohorts of each permutation, respectively.

Comparing change in brain substructure volumes of patients and healthy participants. The outcome variable was the annual volumetric change in each brain substructure. For patients, volumetric data were extracted from the baseline MRI (acquired after surgery and before RT) and from the 2-year follow-up MRI. For control participants, volumetric data were extracted from two MRI scans scheduled 1-2 years apart and the baseline MRI was defined as the initial MRI scan. Linear regression was used to model the annual volumetric change within each treatment group (patients *v* healthy participants), adjusting for baseline volume, age, and sex. Baseline volume was included as a covariate because it differed significantly between patients and healthy participants. All statistical analyses were performed using R version 4.0.2.

RESULTS

Patient Characteristics

A total of 124 patients were eligible for inclusion in the study. Descriptive statistics are presented in Table 1. The median neurocognitive follow-up was 5 years. The number of patients with neurocognitive testing at each time point and individual patient data are shown in Appendix Table A1 and Figure A2 (online only), respectively. Eighty-four patients (68%) were treated on the average-risk arm and received 23.4 Gy CSI. The remainder were treated to ≥ 36 Gy CSI with or without intracranial metastatic boosts. Substructure D_{mean} varied greatly among patients, even within the 23.4 Gy CSI group (Fig 1). Patients treated with ≥ 36 Gy CSI had higher D_{means} across all substructures compared with those treated with 23.4 Gy CSI (Appendix Table A2, online only). Within average-risk patients, sonic hedgehog subgroup (n = 15) was associated with lower right hippocampal D_{mean} compared with nonsonic hedgehog subgroups (n = 62; 34.9 Gy *v* 45.3 Gy, $P = .002$).

Hippocampus and Memory

Appendix Tables A3-A5 (online only) list univariable models for associative memory and working memory. Because PFS was significantly associated with improving associative memory performance on univariable analysis, we analyzed multivariable models of patients with and without PFS separately. In patients without PFS (n = 99), hippocampal D_{mean} was significantly associated with decline in associative memory, after accounting for other significant variables such as age and sex (Table 2). In patients with PFS (n = 19), no clinical or dosimetric variables were associated with the longitudinal trend of associative memory. With respect to working memory, only age and sex had

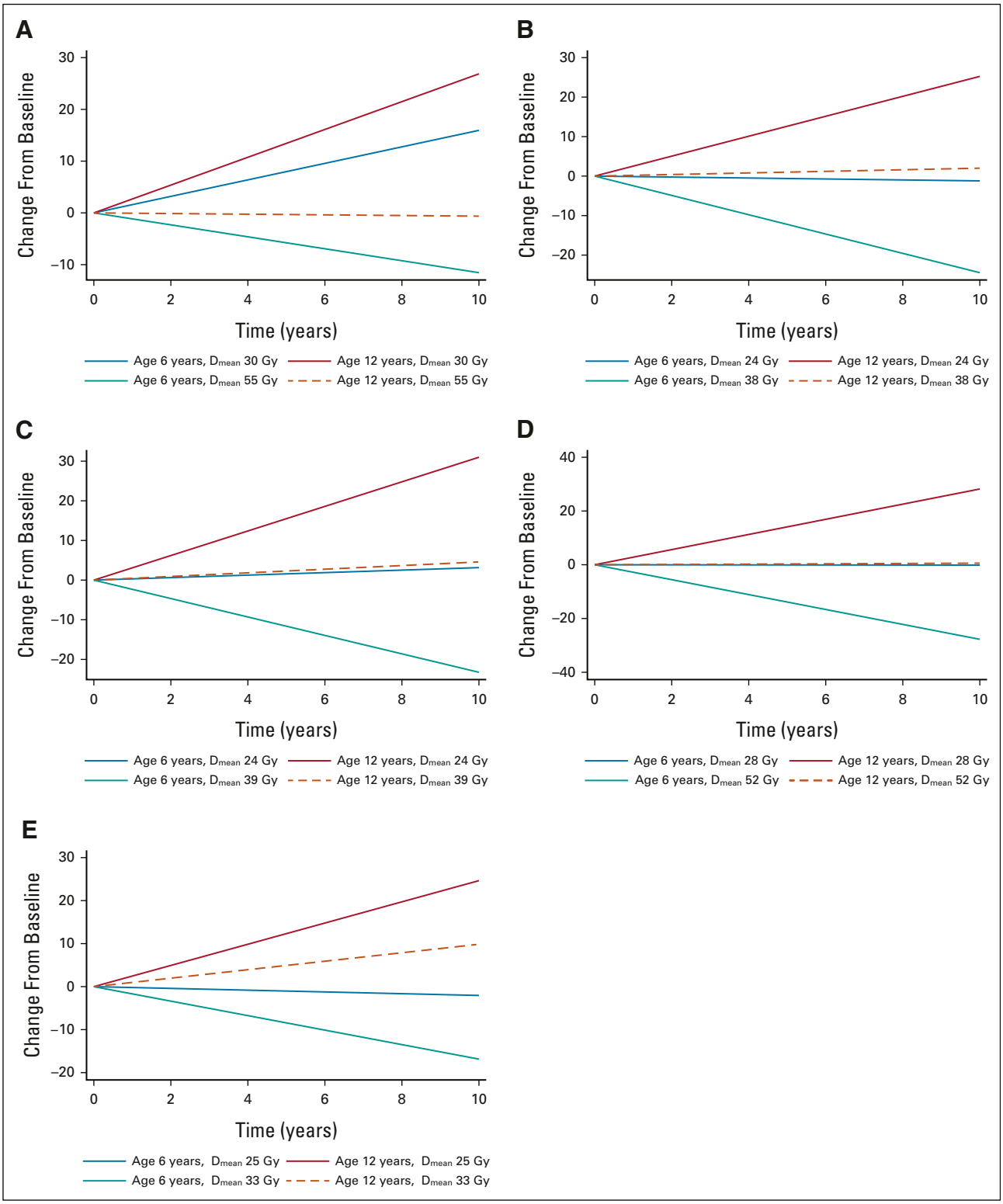

FIG 2. Association between age, brain substructure, and neurocognitive outcomes for (A) the right hippocampus and associative memory, (B) the CC genu and composite processing speed, (C) the CC body and composite processing speed, (D) the CC splenium and composite processing speed, and (E) the right frontal WM and composite processing speed. Data from the left hippocampus and left frontal WM are not shown because the results are similar to those for the contralateral side. The doses displayed represent the fifth and 95th percentiles of the substructure D_{mean} distribution in average-risk patients. CC, corpus callosum; D_{mean}, mean dose; WM, white matter.

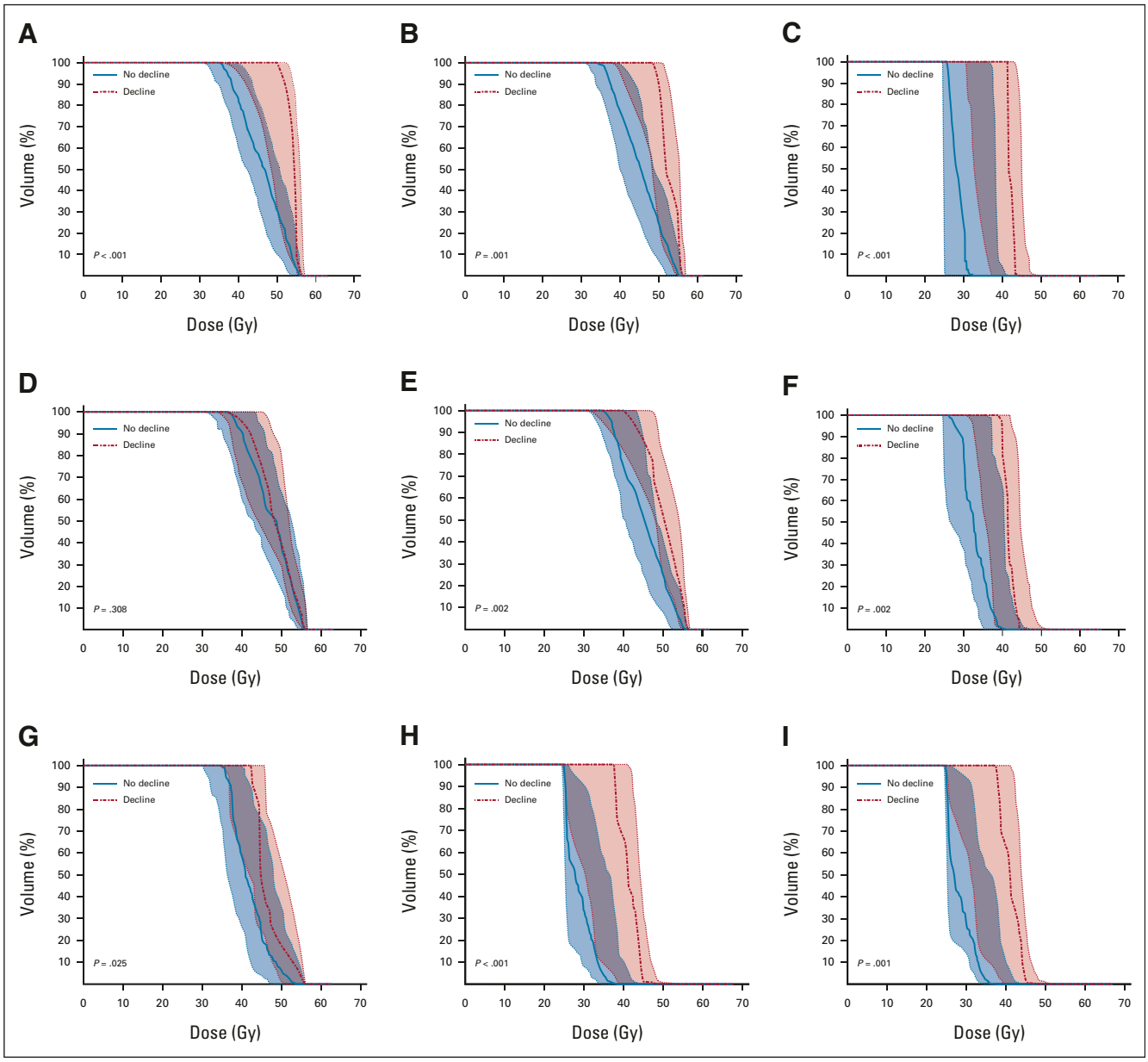

FIG 3. Median population DVHs for patients exhibiting no decline (solid line, blue) compared with patients exhibiting decline (dotted line, red) for the following brain substructures and neurocognitive outcomes: (A) the left hippocampus and associative memory, (B) the right hippocampus and associative memory, (C) the CC genu and composite processing speed, (D) the left hippocampus and working memory, (E) the right hippocampus and working memory, (F) the CC body and composite processing speed, (G) the CC splenium and composite processing speed, (H) the right frontal WM and composite processing speed, and (I) the left frontal WM and composite processing speed. The shaded region represents the 25th-75th percentile. CC, corpus callosum; DVH, dose–volume histogram; WM, white matter.

significant time interactions on multivariable analysis (Table 2). Figure 2A demonstrates how associative memory performance changes with hippocampal D_{mean}, age, and time in patients without PFS.

CC, Frontal WM, and Processing Speed

CC (genu, body, and splenium) and frontal WM D_{means} were associated with declining scores on tests of composite processing and perceptual speed, after accounting for age (Table 2 and Figs 2B-2E). Although hearing loss and hydrocephalus were also associated with declining composite processing and perceptual speed on univariable analysis (Appendix Tables A6 and A7, online only), the associations were not significant on multivariable analysis.

Brain Substructure DVH and Neurocognitive Decline

The number of patients experiencing meaningful declines in associative memory, working memory, composite processing speed, and perceptual speed were 11 (13%), 18 (22%), 17 (18%), and 24 (24%), respectively (Appendix

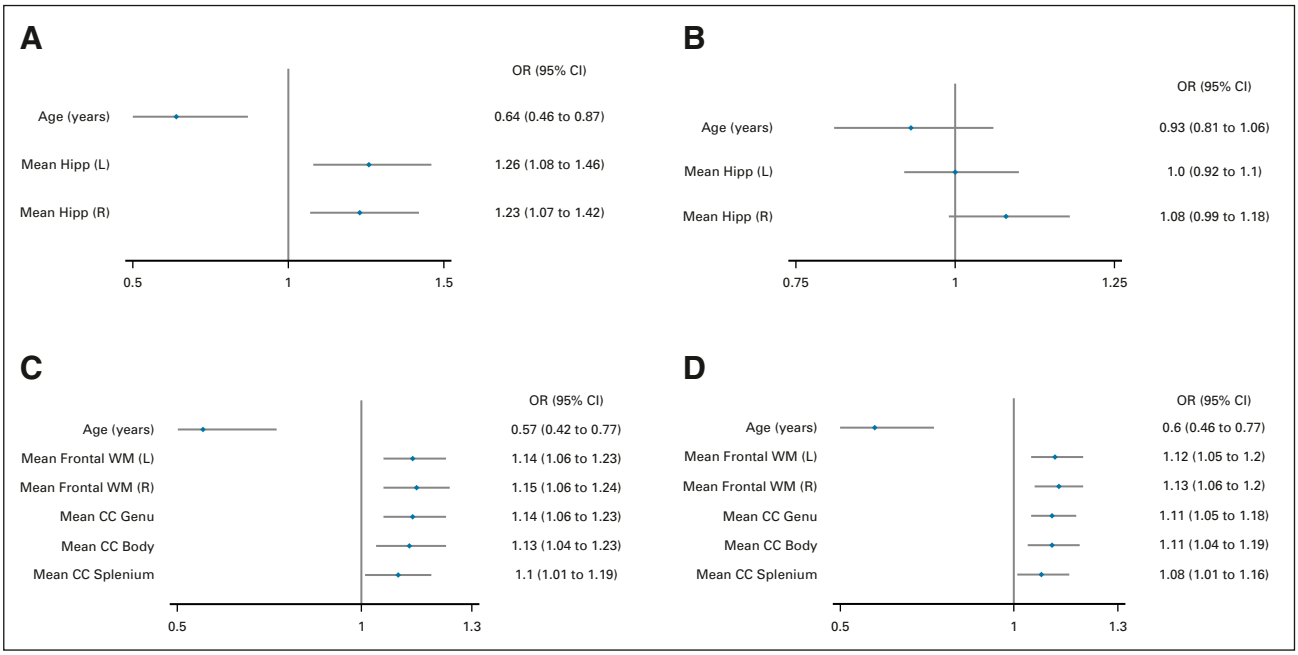

FIG 4. The odds of experiencing neurocognitive decline on the basis of age and D_{mean} with respect to (A) associative memory, (B) working memory, (C) composite processing speed, and (D) perceptual speed. All variables are continuous, and mean doses are represented in Gy. CC, corpus callosum; D_{mean}, mean dose; Hipp, hippocampus; L, left; OR, odds ratio; R, right; WM, white matter.

Table A8, online only). Figure 3 demonstrates population DVHs of patients with and without meaningful decline along with the corresponding *P* values of the permutation tests. The hippocampus median DVH was shifted to the right for patients with a decline in associative memory (left hippocampus: $P < .001$; right hippocampus $P = .001$; Figs 3A and 3B). However, with respect to working memory, the left hippocampus DVH did not differ between patients with and without decline ($P = .308$; Fig 3D), but the right hippocampus DVH did ($P = .002$; Fig 3E). The CC and frontal WM median DVHs were also shifted to the right for patients with a decline in composite processing speed and perceptual speed (all $P \leq .025$; Figs 3C and 3F-3I, and Appendix Fig A3, online only). The odds of decline in associative memory increased by 23%-26% for every 1-Gy increase in hippocampal D_{mean} (Fig 4A). The odds of a decline in composite processing speed and perceptual speed increased by 10%-15% and 8%-12%, respectively, for every 1-Gy increase in CC or frontal WM D_{mean} (Figs 4C and 4D).

Substructure Volumetric Analysis of Patients Versus Healthy Participants

Participant characteristics are listed in Table 1. Appendix Figure A4 (online only) shows baseline and follow-up volumes, acquired 1-2 years from baseline. After accounting for baseline volume, age, and sex, patients demonstrated decreased annual growth in the first 2 years after therapy across all brain substructures when compared with healthy participants (Appendix Table A9, online only).

DISCUSSION

Delivering RT without disrupting cognitive function represents a central dilemma in neuro-oncology. Historically, strategies to mitigate neurocognitive impairment have included reducing the craniospinal dose, reducing the boost volume, and using conformal RT to reduce the dose to normal brain.[20,33,34] There is increasing preclinical and clinical evidence that brain substructures such as the hippocampus, CC, and frontal WM are differentially sensitive to RT injury.[24,35-37] To investigate the relation between brain substructure doses and specific neurocognitive outcomes, we used data from SJMB03. We made four important discoveries: (1) mean substructure dose varied greatly among patients, even within average-risk patients; (2) D_{mean} to certain brain substructures was correlated with longitudinal change of specific neurocognitive functions; (3) substructure DVHs were shifted to the right for patients who experienced clinically meaningful decline, as compared with those who did not; and (4) brain substructure growth was impaired in patients, as compared with healthy participants. Patients also had reduced baseline substructure volumes, potentially explained by hydrocephalus.[38,39] Overall, these data highlight the possibility of cognitively optimizing RT plans, shifting the RT planning paradigm from one that is substructure-naïve to the one that is substructure-informed. This work is particularly timely because hippocampal dose reduction is feasible in the era of proton therapy and tumor bed boosts if the hippocampus is contoured as an organ at risk and proton beam angles are carefully chosen to minimize both hippocampal irradiation

and beam path length. Coupling such technological advances with substructure-informed RT planning may provide the best neurocognitive outcomes.

Declining associative memory performance correlated with increasing hippocampal dose for patients without PFS. The odds of a meaningful decline in associative memory increased by 23%-26% for every 1-Gy increase in hippocampal D_{mean}. For patients with PFS, associative memory performance did not correlate with hippocampal dose and the presence of PFS was associated with improvement in scores over time. This improvement probably reflects the timeline of PFS recovery. The severity of symptoms such as mutism, ataxia, and emotional lability[40] is greatest in the immediate postoperative period; however, symptoms may improve in subsequent months.[41] Unlike associative memory, working memory did not correlate with hippocampal dose after accounting for age and sex. Working memory is highly dependent on the prefrontal cortex,[42] in addition to the hippocampus, and entails short-term active manipulation of information. Associative memory requires learning and recall of information and is more dependent on encoding supported by the hippocampus.

Declining processing speed performance correlated with increasing dose to the CC and frontal WM. The odds of a meaningful decline in composite processing speed and perceptual speed increased by 10%-15% and 8%-12%, respectively, for every 1-Gy increase in CC or frontal WM D_{mean}. Reducing dose to these regions will be difficult without considering new targeting approaches that carve out deep frontal WM from the craniospinal target or reduce the craniospinal dose, as is being tested in patients with nonmetastatic wingless medulloblastoma (ClinicalTrials.gov identifier: NCT01878617, NCT02724579, and NCT04474964). Results from ACNS0331 suggest that novel strategies of dose reduction should be cautiously applied in selected patients on the basis of their molecular genomic risk profile.[43]

This was a retrospective study of prospectively collected data with limitations inherent to the study design (eg, data on handedness were not available). We did not account for practice effects; however, measures used had acceptable test–retest reliability for yearly testing intervals. As doses to different brain regions correlate with one another, we pursued a knowledge-based, hypothesis-driven approach rather than a data-mining approach, limiting our testing to substructures for which there were scientific data correlating the anatomic structure with a neurocognitive function. Finally, intracranial disease burden, independent of RT, may affect neurocognitive outcomes; however, gross disease was either resected or boosted with RT.

This study sets the stage for implementing substructure-informed RT planning in future medulloblastoma protocols. However, more work is needed to understand how RT alters dynamic processes in a child's brain, including the establishment of new neural connections, synaptic pruning, and progressive myelination. Synergizing biologic and clinical understanding of these processes with technological advancements in RT will allow us to deliver the most efficacious therapy with the least amount of damage, improving the lives of medulloblastoma survivors.

AFFILIATIONS

[1]Department of Radiation Oncology, St Jude Children's Research Hospital, Memphis, TN
[2]Department of Radiation Oncology and Molecular Radiation Sciences, Johns Hopkins Medicine, Baltimore, MD
[3]Department of Biostatistics, St Jude Children's Research Hospital, Memphis, TN
[4]Department of Psychology, St Jude Children's Research Hospital, Memphis, TN
[5]Department of Diagnostic Imaging, St Jude Children's Research Hospital, Memphis, TN
[6]Division of Neuro-Oncology, St Jude Children's Research Hospital, Memphis, TN

CORRESPONDING AUTHOR

Sahaja Acharya, MD, Department of Radiation Oncology and Molecular Radiation Sciences, Johns Hopkins Medicine, The Weinberg Building at the Johns Hopkins Kimmel Cancer Center, 401 N. Broadway, Baltimore, MD 21287; e-mail: sachary7@jhmi.edu.

DISCLAIMER

The content is solely the responsibility of the authors and does not necessarily represent the official views of the National Institutes of Health. Any opinions, findings, and conclusions expressed in this material are those of the author(s) and do not necessarily reflect those of the American Society of Clinical Oncology or Conquer Cancer.

SUPPORT

Supported by a 2020 Conquer Cancer—Genentech BioOncology Women Who Conquer Cancer Career Development Award. All the authors received research support from the American Lebanese Syrian Associated Charities (ALSAC) and from Cancer Center Support Grant P30CA021765 from the National Cancer Institute.

CLINICAL TRIAL INFORMATION

NCT00085202 (SJMB3)

AUTHORS' DISCLOSURES OF POTENTIAL CONFLICTS OF INTEREST

Disclosures provided by the authors are available with this article at DOI https://doi.org/10.1200/JCO.21.01480.

DATA SHARING STATEMENT

The data collected on this study cannot be made available to others.

AUTHOR CONTRIBUTIONS

Conception and design: Sahaja Acharya, Wilburn E. Reddick, Amar Gajjar, Heather M. Conklin, Thomas E. Merchant
Administrative support: Amar Gajjar
Provision of study materials or patients: Melissa Gargone, Amar Gajjar, Heather M. Conklin
Collection and assembly of data: Sahaja Acharya, Chuang Wang, Melissa Gargone, Jason M. Ashford, Austin Faught, Wilburn E. Reddick, Zoltan Patay, Amar Gajjar, Heather M. Conklin, Thomas E. Merchant
Data analysis and interpretation: Sahaja Acharya, Yian Guo, Tushar Patni, Yimei Li, Chuang Wang, Lydia Wilson, Austin Faught, Wilburn E. Reddick, Amar Gajjar, Heather M. Conklin, Thomas E. Merchant
Manuscript writing: All authors
Final approval of manuscript: All authors
Accountable for all aspects of the work: All authors

ACKNOWLEDGMENT

The authors thank Keith A. Laycock, PhD, ELS, for scientific editing of the article.

REFERENCES

1. Northcott PA, Robinson GW, Kratz CP, et al: Medulloblastoma. Nat Rev Dis Primers 5:1-20, 2019
2. Palmer SL, Armstrong C, Onar-Thomas A, et al: Processing speed, attention, and working memory after treatment for medulloblastoma: An international, prospective, and longitudinal study. J Clin Oncol 31:3494-3500, 2013
3. Mulhern RK, Palmer SL, Merchant TE, et al: Neurocognitive consequences of risk-adapted therapy for childhood medulloblastoma. J Clin Oncol 23:5511-5519, 2005
4. Brinkman TM, Palmer SL, Chen S, et al: Parent-reported social outcomes after treatment for pediatric embryonal tumors: A prospective longitudinal study. J Clin Oncol 30:4134-4140, 2012
5. Brinkman TM, Ness KK, Li Z, et al: Attainment of functional and social independence in adult survivors of pediatric CNS tumors: A report from the St Jude Lifetime Cohort Study. J Clin Oncol 36:2762-2769, 2018
6. Deng W, Aimone JB, Gage FH: New neurons and new memories: How does adult hippocampal neurogenesis affect learning and memory? Nat Rev Neurosci 11:339-350, 2010
7. Eriksson PS, Perfilieva E, Björk-Eriksson T, et al: Neurogenesis in the adult human hippocampus. Nat Med 4:1313-1317, 1998
8. Boldrini M, Fulmore CA, Tartt AN, et al: Human hippocampal neurogenesis persists throughout aging. Cell Stem Cell 22:589-599.e5, 2018
9. Mizumatsu S, Monje ML, Morhardt DR, et al: Extreme sensitivity of adult neurogenesis to low doses of X-irradiation. Cancer Res 63:4021-4027, 2003
10. Monje ML, Vogel H, Masek M, et al: Impaired human hippocampal neurogenesis after treatment for central nervous system malignancies. Ann Neurol 62: 515-520, 2007
11. Monje ML, Mizumatsu S, Fike JR, et al: Irradiation induces neural precursor-cell dysfunction. Nat Med 8:955-962, 2002
12. Brown PD, Gondi V, Pugh S, et al: Hippocampal avoidance during whole-brain radiotherapy plus memantine for patients with brain metastases: Phase III trial NRG Oncology CC001. J Clin Oncol 38:1019-1029, 2020
13. Acharya S, Wu S, Ashford JM, et al: Association between hippocampal dose and memory in survivors of childhood or adolescent low-grade glioma: A 10-year neurocognitive longitudinal study. Neuro Oncol 21:1175-1183, 2019
14. Goda JS, Dutta D, Krishna U, et al: Hippocampal radiotherapy dose constraints for predicting long-term neurocognitive outcomes: Mature data from a prospective trial in young patients with brain tumors. Neuro Oncol 22:1677-1685, 2020
15. Chapman CH, Nazem-Zadeh M, Lee OE, et al: Regional variation in brain white matter diffusion index changes following chemoradiotherapy: A prospective study using tract-based spatial statistics. PLoS One 8:e57768, 2013
16. Uh J, Merchant TE, Li Y, et al: Effects of surgery and proton therapy on cerebral white matter of craniopharyngioma patients. Int J Radiat Oncol Biol Phys 93: 64-71, 2015
17. Glass JO, Ogg RJ, Hyun JW, et al: Disrupted development and integrity of frontal white matter in patients treated for pediatric medulloblastoma. Neuro Oncol 19: 1408-1418, 2017
18. Brinkman TM, Reddick WE, Luxton J, et al: Cerebral white matter integrity and executive function in adult survivors of childhood medulloblastoma. Neuro Oncol 14:iv25-iv36, 2012 (suppl 4)
19. Perkins S, Acharya S: Radiation therapy to the developing brain: Advanced technology is ready for robust optimization parameters. Neuro Oncol 23:350-351, 2021
20. Gajjar A, Robinson GW, Smith KS, et al: Outcomes by clinical and molecular features in children with medulloblastoma treated with risk-adapted therapy: Results of an International Phase III Trial (SJMB03). J Clin Oncol 39:822-835, 2021
21. Gudrunardottir T, Morgan AT, Lux AL, et al: Consensus paper on post-operative pediatric cerebellar mutism syndrome: The Iceland Delphi results. Childs Nerv Syst 32:1195-1203, 2016
22. The United States Census Bureau: American Community Survey Data. The United States Census Bureau. https://www.census.gov/programs-surveys/acs/data.html
23. Capper D, Jones DTW, Sill M, et al: DNA methylation-based classification of central nervous system tumours. Nature 555:469-474, 2018
24. Redmond KJ, Hildreth M, Sair HI, et al: Association of neuronal injury in the genu and body of corpus callosum after cranial irradiation in children with impaired cognitive control: A prospective study. Int J Radiat Oncol Biol Phys 101:1234-1242, 2018
25. FreeSurfer Software Suite: https://surfer.nmr.mgh.harvard.edu/
26. Schreiber JE, Gurney JG, Palmer SL, et al: Examination of risk factors for intellectual and academic outcomes following treatment for pediatric medulloblastoma. Neuro Oncol 16:1129-1136, 2014
27. McGrew K, RW Woodcock: Technical Manual: Woodcock-Johnson III Tests of Cognitive Abilities. Itasca, IL, Riverside Publishing, 2001
28. Jacobson NS, Truax P: Clinical significance: A statistical approach to defining meaningful change in psychotherapy research. J Consult Clin Psychol 59:12-19, 1991
29. Duff K: Evidence-based indicators of neuropsychological change in the individual patient: Relevant concepts and methods. Arch Clin Neuropsychol 27: 248-261, 2012
30. Camargo A, Azuaje F, Wang H, et al: Permutation-based statistical tests for multiple hypotheses. Source Code Biol Med 3:15, 2008
31. Chen C, Witte M, Heemsbergen W, et al: Multiple comparisons permutation test for image based data mining in radiotherapy. Radiat Oncol 8:293, 2013

32. Dudoit S, Shaffer JP, Boldrick JC: Multiple hypothesis testing in microarray experiments. Stat Sci 18:71-103, 2003
33. Packer RJ, Goldwein J, Nicholson HS, et al: Treatment of children with medulloblastomas with reduced-dose craniospinal radiation therapy and adjuvant chemotherapy: A Children's Cancer Group Study. J Clin Oncol 17:2127-2136, 1999
34. Merchant TE, Schreiber JE, Wu S, et al: Critical combinations of radiation dose and volume predict intelligence quotient and academic achievement scores after craniospinal irradiation in children with medulloblastoma. Int J Radiat Oncol Biol Phys 90:554-561, 2014
35. Palmer SL, Glass JO, Li Y, et al: White matter integrity is associated with cognitive processing in patients treated for a posterior fossa brain tumor. Neuro Oncol 14:1185-1193, 2012
36. Parihar VK, Limoli CL: Cranial irradiation compromises neuronal architecture in the hippocampus. Proc Natl Acad Sci USA 110:12822-12827, 2013
37. Wang S, Wu EX, Qiu D, et al: Longitudinal diffusion tensor magnetic resonance imaging study of radiation-induced white matter damage in a rat model. Cancer Res 69:1190-1198, 2009
38. Lane JI, Luetmer PH, Atkinson JL: Corpus callosal signal changes in patients with obstructive hydrocephalus after ventriculoperitoneal shunting. Am J Neuroradiol 22:158-162, 2001
39. Chen L-J, Wang Y-J, Chen J-R, et al: Hydrocephalus compacted cortex and hippocampus and altered their output neurons in association with spatial learning and memory deficits in rats. Brain Pathol 27:419-436, 2017
40. Robertson PL, Muraszko KM, Holmes EJ, et al: Incidence and severity of postoperative cerebellar mutism syndrome in children with medulloblastoma: A prospective study by the Children's Oncology Group. J Neurosurg 105:444-451, 2006
41. Gudrunardottir T, Sehested A, Juhler M, et al: Cerebellar mutism: Review of the literature. Childs Nerv Syst 27:355-363, 2011
42. D'Esposito M, Postle BR: The cognitive neuroscience of working memory. Annu Rev Psychol 66:115-142, 2015
43. Michalski JM, Janss AJ, Vezina LG, et al: Children's Oncology Group phase III trial of reduced-dose and reduced-volume radiotherapy with chemotherapy for newly diagnosed average-risk medulloblastoma. J Clin Oncol 39:2685-2697, 2021

AUTHORS' DISCLOSURES OF POTENTIAL CONFLICTS OF INTEREST

Association Between Brain Substructure Dose and Cognitive Outcomes in Children With Medulloblastoma Treated on SJMB03: A Step Toward Substructure-Informed Planning

The following represents disclosure information provided by authors of this manuscript. All relationships are considered compensated unless otherwise noted. Relationships are self-held unless noted. I = Immediate Family Member, Inst = My Institution. Relationships may not relate to the subject matter of this manuscript. For more information about ASCO's conflict of interest policy, please refer to www.asco.org/rwc or ascopubs.org/jco/authors/author-center.

Open Payments is a public database containing information reported by companies about payments made to US-licensed physicians (Open Payments).

Lydia Wilson
Honoraria: Elekta

Amar Gajjar
Consulting or Advisory Role: Roche/Genentech, QED Therapeutics, Day One Therapeutics
Research Funding: Genentech (Inst), Kazia Therapeutics (Inst)

Thomas E. Merchant
Honoraria: Varian Medical Systems
Travel, Accommodations, Expenses: Philips Healthcare

No other potential conflicts of interest were reported.

APPENDIX

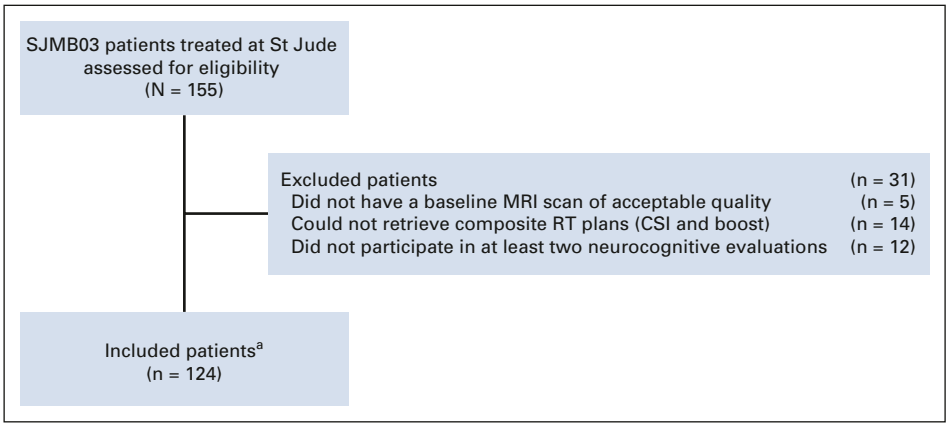

FIG A1. Flow diagram. [a]There were no statistically significant differences in age, sex, and risk group when comparing SJMB03 patients excluded from this study with those included in this study (age, $P = .107$; sex, $P = .942$; risk group, $P = .872$). CSI, craniospinal irradiation; MRI, magnetic resonance imaging; RT, radiation.

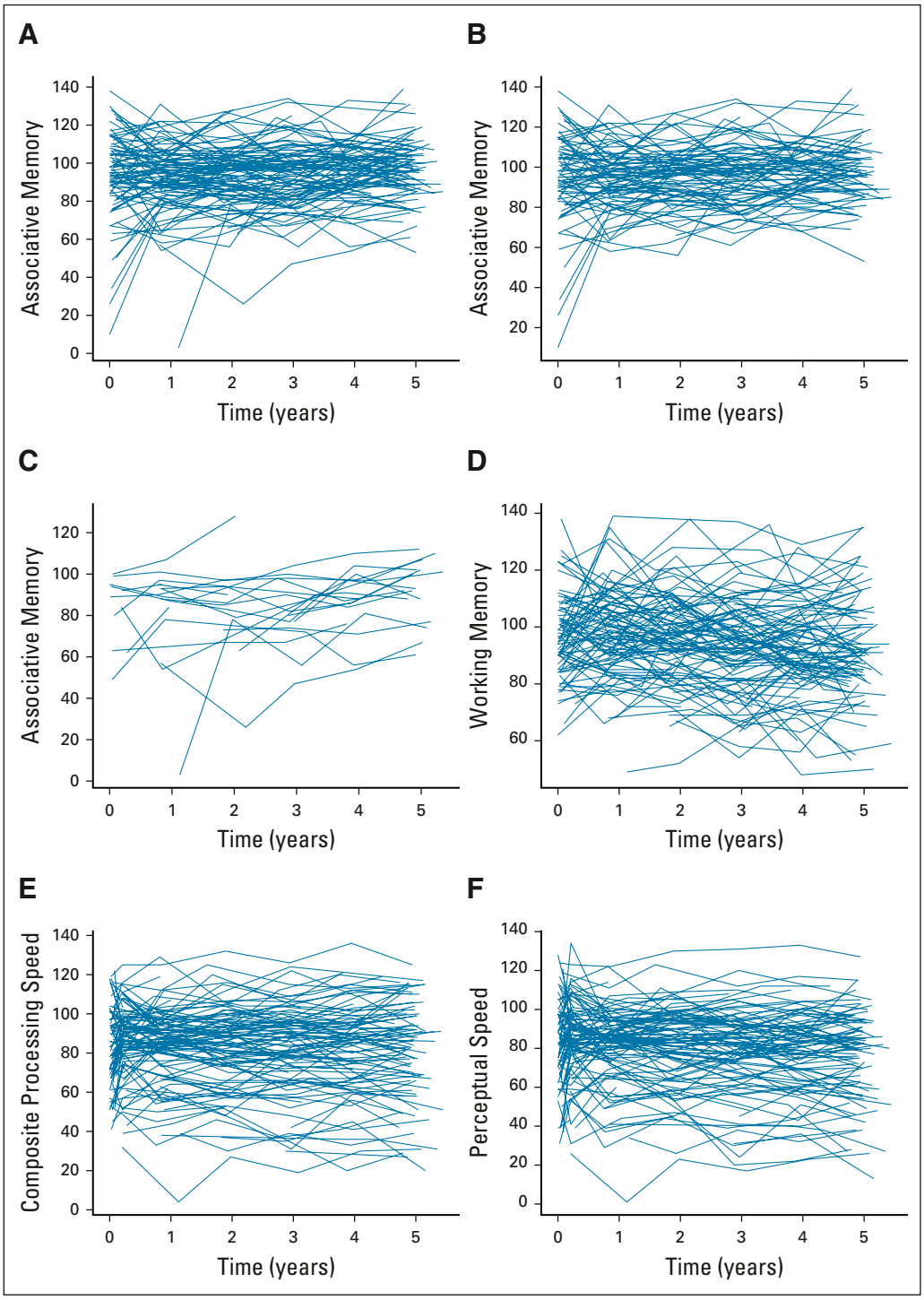

FIG A2. Raw individual patient data for (A) associative memory, (B) associative memory for patients without PFS, (C) associative memory for patients with PFS, (D) working memory, (E) composite processing speed, and (F) perceptual speed. PFS, posterior fossa syndrome.

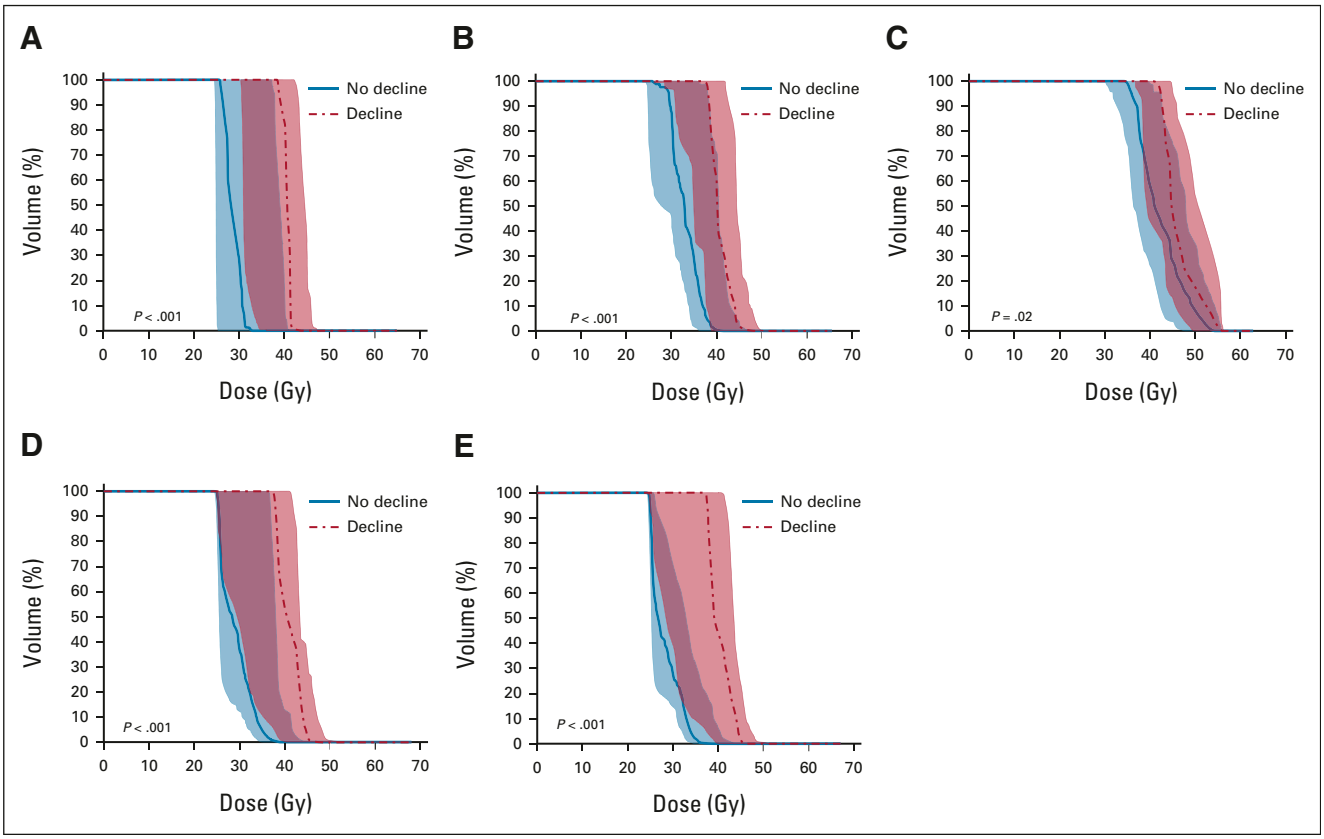

FIG A3. Median population DVHs for patients exhibiting no decline (solid line, blue) compared with patients exhibiting decline (dotted line, red) in perceptual speed for the following brain substructures: (A) the CC genu, (B) the CC body, (C) the CC splenium, (D) the left frontal WM, and (E) the right frontal WM. The shaded region represents the 25th-75th percentile. CC, corpus callosum; DVH, dose–volume histogram; WM, white matter.

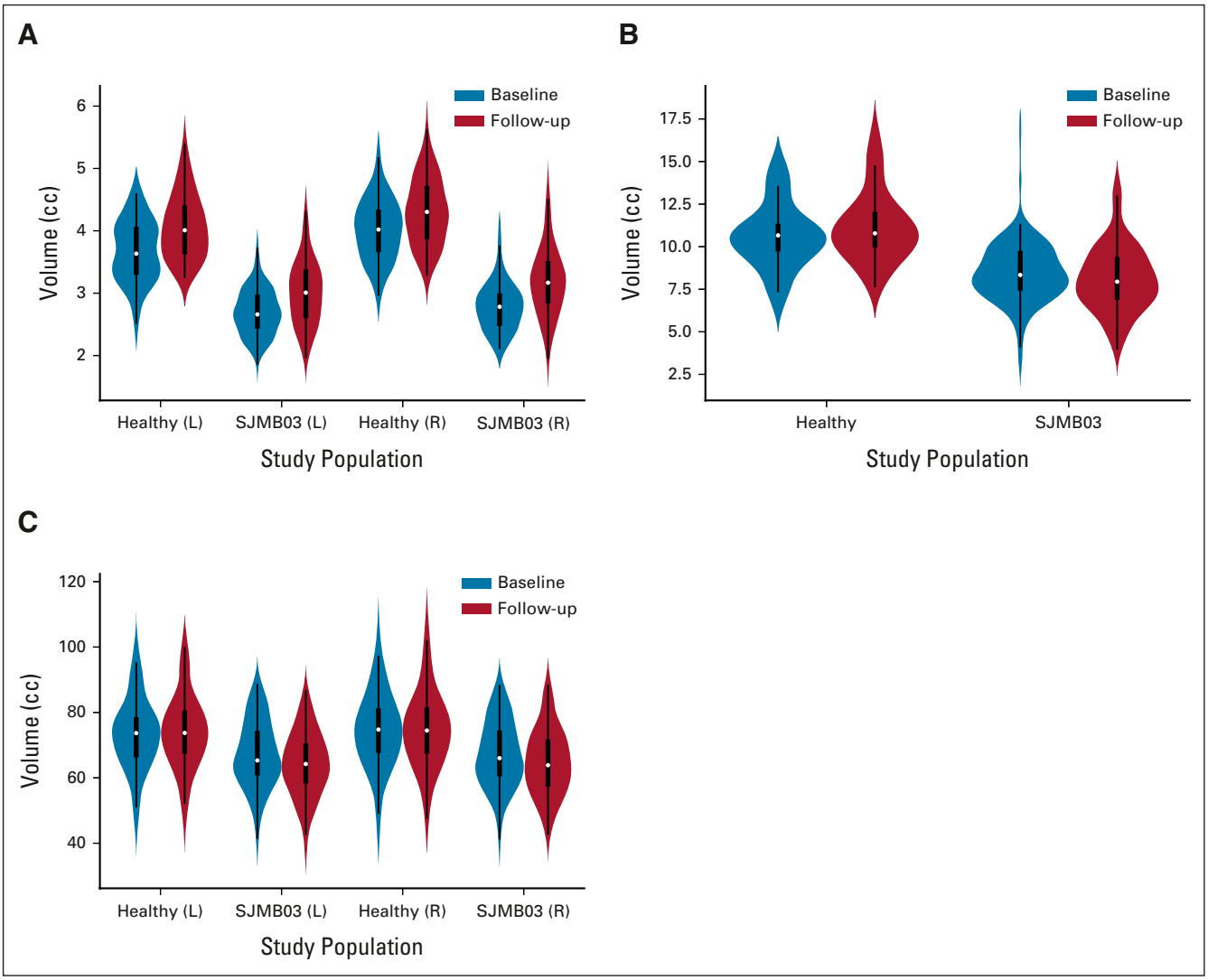

FIG A4. Violin plots comparing patient (SJMB03) and healthy participant (healthy) substructure volumes for (A) the hippocampus, (B) the CC, and (C) the frontal WM. The follow-up time was 1-2 years after the baseline time point. CC, corpus callosum; L, left; R, right; WM, white matter.

TABLE A1. No. of Patients With Neurocognitive Testing at Each Time Point

		Months				
Neurocognitive Measure	**Baseline**	**12**	**24**	**36**	**48**	**60**
Associative memory	98	102	88	93	86	80
Working memory	88	95	85	93	84	79
Visual matching	108	101	88	93	84	80
Processing speed	108	99	86	90	84	78

TABLE A2. Association Between Substructure D_{mean} and Risk Group

Substructure	Average Risk (median, range [Gy])	High Risk (median, range [Gy])	P[a]
Left frontal WM D_{mean}	27.76, 24.25-55.93	42.21, 37.85-50	< .001
Right frontal WM D_{mean}	27.79, 24.28-55.37	42.37, 38.3-46.74	< .001
Left hippocampus D_{mean}	45.26, 29.78-59.02	52.66, 39.83-61.4	< .001
Right hippocampus D_{mean}	43.89, 26.32-58.89	51.92, 40.89-57.54	< .001
CC genu D_{mean}	25.96, 23.77-62.34	42.26, 37.62-56.04	< .001
CC body D_{mean}	31.79, 24-63.29	43.36, 37.65-48.81	< .001
CC splenium D_{mean}	41.44, 25.16-60.29	49.56, 38.19-60.23	< .001

Abbreviations: CC, corpus callosum; D_{mean}, mean dose; WM, white matter.
[a]Wilcoxon rank-sum test.

TABLE A3. Parameter Estimates of Univariable Linear Mixed Models of Associative Memory Over Time

Variable	No. of Patients	No. of Observations	Estimate	SE	P
Associative memory	121	547			
Left hippocampus					
Intercept			89.530	11.305	< .001
Time			5.342	2.087	.011
Left D_{mean}			0.051	0.238	.829
Left D_{mean} × time			–0.090	0.044	.043
Right hippocampus					
Intercept			92.952	9.768	< .001
Time			5.479	1.927	.005
Right D_{mean}			–0.023	0.212	.915
Right D_{mean} × time			–0.096	0.042	.024
Age					
Intercept			92.450	3.616	< .001
Time			–0.617	0.708	.384
Age			–0.051	0.332	.877
Age × time			0.171	0.063	.007
Sex					
Intercept			88.415	1.823	< .001
Time			1.664	0.354	< .001
Sex			9.246	2.989	.002
Sex × time			–1.388	0.579	.017
PFS					
Intercept			94.645	1.548	< .001
Time			0.862	0.303	.005
PFS			–17.291	3.827	< .001
PFS × time			2.126	0.783	.007

NOTE. Only models with significant time interactions are shown. For dose variables, only D_{mean} models are shown.
Abbreviations: D_{mean}, mean dose; PFS, posterior fossa syndrome.

TABLE A4. Parameter Estimates of Univariable Linear Mixed Models of Associative Memory Over Time in Patients Without PFS

Variable	No. of Patients	No. of Observations	Estimate	SE	*P*
Associative memory (no PFS)	99	453			
Left hippocampus					
Intercept			73.156	11.143	< .001
Time			6.939	2.113	.001
Left D_{mean}			0.462	0.237	.053
Left D_{mean} × time			–0.132	0.046	.004
Right hippocampus					
Intercept			83.158	9.759	< .001
Time			6.839	1.957	.001
Right D_{mean}			0.255	0.214	.234
Right D_{mean} × time			–0.134	0.043	.002
Age					
Intercept			99.020	3.695	< .001
Time			–1.404	0.745	.060
Age			–0.417	0.329	.207
Age × time			0.212	0.064	.001
Sex					
Intercept			90.390	1.871	< .001
Time			1.346	0.381	< .001
Sex			10.698	2.968	< .001
Sex × time			–1.235	0.605	.042

NOTE. Only models with significant time interactions are shown. For dose variables, only D_{mean} models are shown.
Abbreviations: D_{mean}, mean dose; PFS, posterior fossa syndrome.

TABLE A5. Parameter Estimates of Univariable Linear Mixed Models of Working Memory Over Time

Variable	No. of Patients	No. of Observations	Estimate	SE	*P*
Working memory	117	524			
Right hippocampus					
Intercept			97.886	9.528	< .001
Time			3.389	1.890	.074
Right D_{mean}			–0.047	0.207	.819
Right D_{mean} × time			–0.087	0.041	.035
Age					
Intercept			98.546	3.668	< .001
Time			–3.083	0.720	< .001
Age			–0.245	0.329	.458
Age × time			0.237	0.063	< .001
Sex					
Intercept			93.798	1.840	< .001
Time			–0.060	0.349	.864
Sex			4.889	2.954	.100
Sex × time			–1.300	0.561	.021

NOTE. Only models with significant time interactions are shown. For dose variables, only D_{mean} models are shown.
Abbreviation: D_{mean}, mean dose.

TABLE A6. Parameter Estimates of Univariable Linear Mixed Models of Composite Processing Speed Over Time

Variable	No. of Patients	No. of Observations	Estimate	SE	*P*
Processing speed	122	629			
CC genu					
Intercept			73.373	7.929	< .001
Time			7.013	0.937	< .001
Genu D_{mean}			0.256	0.234	.276
Genu D_{mean} × time			–0.203	0.028	< .001
CC body					
Intercept			74.658	9.547	< .001
Time			7.414	1.138	< .001
Body D_{mean}			0.201	0.265	.451
Body D_{mean} × time			–0.200	0.032	< .001
CC splenium					
Intercept			73.841	11.106	< .001
Time			6.265	1.322	< .001
Splenium D_{mean}			0.186	0.255	.467
Splenium D_{mean} × time			–0.139	0.031	< .001
Left frontal WM					
Intercept			69.096	8.688	< .001
Time			7.458	1.027	< .001
Left D_{mean}			0.386	0.259	.139
Left D_{mean} × time			–0.218	0.031	< .001
Right frontal WM					
Intercept			69.515	8.732	< .001
Time			7.603	1.027	< .001
Right D_{mean}			0.376	0.262	.153
Right D_{mean} × time			–0.223	0.031	< .001
Age					
Intercept			84.915	4.458	< .001
Time			–4.701	0.552	< .001
Age			–0.291	0.414	.484
Age × time			0.488	0.049	< .001
Hearing loss					
Intercept			81.490	2.053	< .001
Time			0.679	0.263	.010
Hearing loss			1.381	4.941	.780
Hearing loss × time			–1.463	0.571	.011
Hydrocephalus					
Intercept			84.152	2.584	< .001
Time			1.266	0.334	< .001
Hydrocephalus			–4.414	3.642	.228
Hydrocephalus × time			–1.726	0.465	< .001

NOTE. Only models with significant time interactions are shown. For dose variables, only D_{mean} models are shown.
Abbreviations: CC, corpus callosum; D_{mean}, mean dose; WM, white matter.

TABLE A7. Parameter Estimates of Univariable Linear Mixed Models of Perceptual Speed Over Time

Variable	No. of Patients	No. of Observations	Estimate	SE	*P*
Perceptual speed	122	644			
CC genu					
Intercept			68.884	7.828	< .001
Time			6.334	0.996	< .001
Genu D_{mean}			0.389	0.232	.096
Genu D_{mean} × time			–0.215	0.030	< .001
CC body					
Intercept			69.981	9.443	< .001
Time			6.679	1.208	< .001
Body D_{mean}			0.329	0.263	.212
Body D_{mean} × time			–0.209	0.034	< .001
CC splenium					
Intercept			70.918	10.974	< .001
Time			5.553	1.403	< .001
Splenium D_{mean}			0.250	0.252	.322
Splenium D_{mean} × time			–0.147	0.032	< .001
Left frontal WM					
Intercept			64.711	8.560	< .001
Time			6.793	1.088	< .001
Left D_{mean}			0.516	0.255	.045
Left D_{mean} × time			–0.230	0.033	< .001
Right frontal WM					
Intercept			64.700	8.607	< .001
Time			6.985	1.088	< .001
Right D_{mean}			0.519	0.258	.046
Right D_{mean} × time			–0.236	0.033	< .001
Age					
Intercept			85.598	4.397	< .001
Time			–5.828	0.587	< .001
Age			–0.380	0.408	.354
Age × time			0.499	0.052	< .001
Hearing loss					
Intercept			81.231	2.024	< .001
Time			–0.404	0.278	.146
Hearing loss			2.154	4.872	.659
Hearing loss × time			–1.337	0.607	.028
Hydrocephalus					
Intercept			83.791	2.559	< .001
Time			0.198	0.355	.578
Hydrocephalus			–4.029	3.610	.266
Hydrocephalus × time			–1.670	0.492	.001

NOTE. Only models with significant time interactions are shown. For dose variables, only D_{mean} models are shown.
Abbreviations: CC, corpus callosum; D_{mean}, mean dose; WM, white matter.

TABLE A8. Patient Scores at Baseline and at Last Neurocognitive FU

Neurocognitive Measure	No. of Patients (%)	Median Score at Baseline (range)	Median Score at Last FU (range)	Median FU Time[a] (range)
Associative memory				
Decline	11 (13)	115 (86-138)	87 (53-120)	59.6 (9.8-65.3)
No decline	76 (87)	93 (10-128)	100 (61-139)	58.9 (9.9-65.0)
Working memory				
Decline	18 (22)	103 (80-125)	83 (53-105)	57.8 (24.2-65.3)
No decline	62 (78)	92 (62-138)	97.5 (65-135)	59.0 (9.8-65.0)
Composite processing speed				
Decline	17 (18)	97 (55-110)	72 (29-94)	58.9 (35.0-65.3)
No decline	80 (82)	81 (32-119)	91 (31-125)	58.4 (9.7-65.0)
Perceptual speed				
Decline	24 (24)	96.5 (59-113)	69.5 (27-93)	59.6 (10.4-65.3)
No decline	75 (76)	82 (26-124)	86 (26-127)	58.3 (9.7-65.0)

Abbreviations: FU, follow-up; RT, radiation.

[a]FU time is measured in months from the start of RT to the last neurocognitive test.

TABLE A9. Parameter Estimates From Linear Models That Investigate the Association Between the Annual Volumetric Change From Baseline and Baseline Volume, Age at Diagnosis, Sex, and Group (patients *v* healthy participants)

Variable	No. of Patients/Healthy Participants	No. of Observations	Estimate	SE	*P*
Left hippocampus	101/82	183			
Intercept			1.248	0.173	< .001
Baseline			–0.310	0.044	< .001
Age			0.009	0.004	.020
Sex (female *v* male)			–0.104	0.038	.007
Group (patients *v* healthy participants)			–0.310	0.059	< .001
Right hippocampus	101/82	183			
Intercept			1.038	0.186	< .001
Baseline			–0.247	0.044	< .001
Age			0.009	0.004	.023
Sex (female *v* male)			–0.061	0.038	.110
Group (patients *v* healthy participants)			–0.219	0.067	.001
CC	101/82	183			
Intercept			2.721	0.395	< .001
Baseline			–0.248	0.034	< .001
Age			0.035	0.014	.012
Sex (female *v* male)			–0.521	0.129	< .001
Group (patients *v* healthy participants)			–0.953	0.151	< .001
Left frontal WM	99/82	181			
Intercept			17.965	2.191	< .001
Baseline			–0.299	0.028	< .001
Age			0.418	0.061	< .001
Sex (female *v* male)			–3.525	0.594	< .001
Group (patients *v* healthy participants)			–2.257	0.624	< .001
Right frontal WM	99/82	181			
Intercept			15.588	2.250	< .001
Baseline			–0.271	0.028	< .001
Age			0.446	0.062	< .001
Sex (female *v* male)			–3.331	0.607	< .001
Group (patients *v* healthy participants)			–1.919	0.643	.003

NOTE. Annual volumetric change is calculated using data from the first 2 years after the baseline MRI scan. For patients, the baseline MRI scan is defined as the postoperative MRI before the start of RT therapy. For healthy participants, the baseline MRI scan is the first MRI scan to be acquired.

Abbreviations: CC, corpus callosum; MRI, magnetic resonance imaging; RT, radiation; WM, white matter.